ICAS-88-3.7R

TRANSONIC SHOCK BOUNDARY LAYER INTERACTION WITH PASSIVE CONTROL

S. Raghunathan and S.T. McIlwain
Department of Mechanical and Manufacturing, Aeronautical, and Chemical Engineering
The Queen's University of Belfast,
Belfast BT9 5AG. United Kingdom

Abstract

Passive control experiments were conducted on a wall mounted part section supercritical aerofoil at R_θ = 5,700 and in the shock Mach number range $1.2 < M_{SO} < 1.34$. The porosity of the porous surface was 2.14%. The results of the experiments were in agreement with earlier experiments on a wall mounted circular arc model at R_θ = 10,000. Some of the results were in disagreement with experiments conducted by Nagamatsu et al on the same supercritical aerofoil model at $R_\theta \simeq 3{,}000$. It is suggested that detailed experiments should be conducted on a large scale model to fully understand the mechanism and benefits of passive controlled shock boundary layer interaction.

Nomenclature

C_D	profile drag coefficient
C_p	pressure coefficient
c	model chord length
d	diameter of the holes
H	boundary layer shape factor
h	tunnel height
h_c	cavity depth
L*	interaction length
M	free stream Mach number
M_{SO}	shock Mach number, solid model
p_o	total pressure in the wake
$p_{o\infty}$	total pressure in the free stream
p	porosity, ratio of open area to model area
U_∞	velocity at the edge of the boundary layer
u	local velocity in the boundary layer
t	model thickness
x	distance along the model chord line
X_{so}	shock position, solid model
y	distance normal to the model chord line
δ	boundary layer thickness at $u = 0.995\ U_\infty$
δ^*	boundary layer displacement thickness
θ	boundary layer momentum thickness

1. Introduction

Transonic flow over an aerofoil contains supersonic regions embedded in a subsonic flow. The supersonic flow invariably terminates in a shock wave which results in a wave drag. the interaction between a shock wave and boundary layer may lead to boundary layer separation which constitutes an additional drag. Unsteady pressures associated with a shock boundary layer interaction can also induce high levels of buffeting.

Postponement of Mach number at which significant increases in drag and buffet occurs would need the control of shock boundary layer interaction and one of the possible control techniques which appears to be promising is the passive control of shock boundary layer interaction[1-10] (PCSB) schematically illustrated in Fig. 1. The concept consists of a porous surface and a cavity located at the foot of the shock. The natural static pressure rise across the shock sets up a recirculating airflow, the upstream effect which would thicken the approaching boundary layer, softens the shock system reducing the wave drag. It could be conceivable that suction of the boundary layer behind the shock can also control separation. Both the experimental[1-9] and theoretical[10] investigations have shown that passive control of shock boundary layer interaction can reduce drag and alleviate buffeting. But there are several aspects of PCSB which are yet to be understood. These are for example (i) the mechanism by which drag reduction is achieved (ii) the type of porous surface required for maximum drag reduction (iii) scale effect on PCSB and (iv) the minimum shock strength required for a significant drag reduction.

Some of the earlier work on passive control by the author[5-8] on a part section circular arc model mounted on the roof of a small transonic tunnel suggests that (i) inclined holes are better than normal holes (ii) the shock Mach number $M_{SO} > 1.3$ for significant drag reduction. The drag reduction obtained in those experiments was attributed to the softening of the shock wave by the PCSB and a consequent reduction in entropy changes across the shock. This was in contrast to the results of Refs. 1,2,3 which suggest that the drag reduction obtained in PCSB is primarily due to the reduced separation i.e. reduced viscous losses. The

experiments of the author were conducted at a high value of $R_\theta = 10^4$ with a thick boundary layer at the foot of the shock and it is possible that the results could have been affected by flow separation at the trailing of the circular arc model. The experiments of Nagamatsu et al[1-3] were conducted on a supercritical aerofoil with relatively thin boundary layer at the foot of the shock ($R_\theta \simeq 3,000$).

In this paper results are presented of experiments on PCSB performed with the same wall mounted aerofoil as Ref. 2 with a boundary layer bleed upstream of the aerofoil which resulted in the boundary layer momentum thickness at the foot of the shock of $R_\theta = 5,700$. The investigations also included tests with porous surfaces made of inclined holes and normal holes and the shock Mach number range of $1.2 < M_S < 1.34$.

2. Test facility, models and test conditions

Experiments were conducted in a 101mm square blow down transonic tunnel with an atmospheric intake. The test section (Fig. 2) had closed side walls and a slotted floor with two slots covered with screens. The porosity of the floor was 9.6%.

The model was NASA 14% thick part section supercritical aerofoil[1,2], which had the same profile given in Ref. 1. The model chord length was 101mm. The model blockage was t/h = 0.07 and the effective chord to tunnel height c/h = 0.5. The generally recommended values of t/h < 1.5%. However these were not regarded as critical as the measurements were only of comparative nature. Boundary layer bleed was applied to both the side walls and the tunnel roof at a distance 0.5c upstream of the model leading edge which resulted in a value of $R_\theta = 5,700$ and $\delta^*/c = 5 \times 10^{-3}$ at the foot of the shock. This value of R_θ is about twice the estimated value for the experiments of Refs. 1 - 3 but nevertheless the shock boundary layer interaction in both cases is likely to be dominated viscous forces. One solid model and two porous models were tested. For the porous models the porous region consisted of 1mm diameter holes located in the region $0.65 < x_p < 0.80$. The holes were normal to the surface for the normal holes model (NH) and inclined at 60^0 to the normal to the chord lines for the forward facing holes model (FFH).

The ratio of diameter of the holes d to the boundary layer displacement thickness upstream of the shock was $\frac{d}{\delta^*} = 2$. The porosity of the models, based on the open area to total model plan form area was p = 2.14% The cavity depth beneath the porous surface had an average depth of $h_c = 6.20$mm resulting in a value of $h_c/\delta^* = 12.5$. All the models had pressure orifices located at 5mm intervals up to mid chord position and 2.5mm intervals between the mid chord and the trailing edge.

Shock Mach numbers of $M_{SO} = 1.2$, 1.275, 1.3 and 1.34 with reference to the solid model (SM) were chosen as test conditions.

The shock position was within the range $0.6 < X_{so}/c < 0.75$.

A Scanivalve with a pressure storage box was used for the pressure measurements. Wake traverses were performed at a position x/c = 1.1 on the centre line of the model. A pitot tube with a front opening of 1.3 mm x 0.25 mm and a Druck PDCR 32 transducer was used for this purpose. Shadowgraph pictures were taken for the three test conditions on all three models.

The free stream Mach number was based on a side wall pressure measurement 2 chord upstream of the model leading edge. The Mach number in the tunnel was controlled by a shock located downstream of the test section. (Fig. 3)

It should be emphasised that the model test did not fulfil the circulation and trailing conditions of a lifting aerofoil and therefore was intended only as a comparative test.

3. Results and discussions

Comparison of pressure distribution on the model with and without passive control for shock Mach numbers of $M_{SO} = 1.2$, 1.27, 1.30 and 1.34 shown in Figs. 4a, 4b, 4c, and 4d respectively indicate the following general features of passive controlled shock boundary layer intereaction.

(i) Passive control reduces the pressure gradients in the interaction region. The only sharp changes in the pressure distribution are near the beginning and end of the porous region. The peak negative pressure is reduced.

(ii) a single shock wave is split into two shock waves. (This was confirmed by Schlieren photographs.)

(iii) Passive control increases the interaction length, which is the distance between the position of the peak Mach number and Mach number of unity. This would suggest increased communication in the interaction region and therefore increased upstream influence.

(iv) Passive control also produces a hump in the pressure distribution in the interaction region. This would indicate a change in effective geometry possibly due to a recirculating airflow in the porous region.

(v) Passive control reduces trailing edge pressures.

(vi) Passive control is sensitive to hole inclination. The changes produced in the pressure distribution are larger with Forward facing holes when compared with normal holes.

Features (i) to (vi) are consistent with earlier works by the author on a wall mounted circular arc model. Features (i) to (v) agree with the theoretical predictions by Chen et al[10] for RAE 2822 aerofoil at relatively higher Reynolds number shown (Fig. 5). There is a disagreement of present results with those of Nagamatsu et al[1-3] as far as feature (v). Nagamatsu et al[13] results (Fig. 6) indicate no change in the trailing edge pressure with the application of passive control. Features (i), (ii), and (v) are in disagreement with the results of Krogaman et al[4] (Fig. 7a) whose experiments were the only experiments performed on a lifting aerofoil, with porous surface made of slots and with a very low porosity of 0.3%

Further it is interesting to observe from Krogamann et al[4] experiments that significant changes in the pressure distribution was obtained even when the slots were downstream of the original shock position, Fig. 7b.

The effect of passive control with normal holes and inclined holes is shown in Figs. 8a and 8b respectively. On a porous surface the shock system is spread with the leading edge shock wave which is oblique and anchored nearer the beginning of the porous region. The trailing edge shock wave is nearly normal and generally within the porous region for normal holes (Fig. 8a) and near the end of the porous region for the forward facing holes (Fig. 8b). This feature is in general agreement with earlier work on a circular arc model[5,8] and the observations by Nagamatsu et al[1-3] (Fig. 9). The spread of the shock system on a porous surface has also been predicted theoretically[10].

The relative losses in a shock boundary layer interaction can be understood from a plot downstream of the interaction of stagnation pressures $p_o/p_{o\infty}$ vs distance normal to the surface y/c. Within the boundary layer and close to the surface the losses are essentially viscous losses whereas outside the boundary layer the losses are due to entropy increases across the shock wave. An integral value given by

$$I_w = \int_o^\infty (1-p_o/p_{o\infty})d(y/c)$$

is a measure of the loss of total pressure due to shock boundary layer interaction.

Comparison of the measurements of stagnation pressure profiles in the wake 10% chord downstream of the model trailing edge are shown in Figs. 10a, 10b and 10c, for three shock Mach numbers M_{SO} = 1.2, 1.3 and 1.37 respectively. The boundary layer thickness δ corresponds to a value of y/c typically of 0.12. The results of the porous surface made of normal holes shows that for all shock Mach numbers passive control increases the viscous losses within the boundary layer but decreases the entropy increase across the shock wave. This result is consistent with those of earlier tests on a circular arc aerofoil[5,8] and theoretical prediction by Chen et al[10]. The experiments of Nagamatsu et al[1-3] showed that passive control can also reduce viscous losses within the boundary layer (Fig. 11). Reduction in viscous losses within the boundary layer was obtained in the present experiment with forward facing holes but only at relatively high shock Mach number (Fig. 10c). Similar results were obtained in earlier experiments on circular arc model[5,8].

The variations with Mach number of boundary layer displacement thickness δ^*_w/c, shape factor H_w and integral value of total pressure losses I_w based on the measurements 10% chord downstream of the model trailing edge, are shown in Figs. 12a, 12b and 12c respectively.

For the solid model δ^*/c and H_w (Figs. 12a and 12b) increase considerably at a shock Mach number $M_{SO} \simeq 1.3$ showing the significant effect of shock induced separation. For $M_{SO} < 1.3$, passive control thickens the boundary layer and makes the boundary layer less full possibly due to the dominating effect of blowing over suction in the interaction region. For $M_{SO} > 1.3$ and with passive control with normal holes the measured values of δ^*w/c and H_w are only slightly higher than those corresponding to the solid model. Theoretical calculations on the RAE 2822 aerofoil[10] and some boundary layer measurements on a circular arc profile[7] also show that passive control thickens the boundary layer. Only the forward facing holes model at a high shock strength shows some suction effects. It could be argued that the boundary layer development in the subsonic region downstream of the aerofoil is a function of upstream boundary layer influence. With passive control the boundary layer approaching the shock interaction is thicker and, when subjected to a shock interaction, even with a softened shock system, takes a long distance to rehabilitate itself and is less resistant to separation.

This would result in a thicker boundary layer downstream of the interaction. This argument would support the predicted[10] and measured[5,8] values of trailing edge pressure, shown to be lower with the passive control. The thickening of the boundary layer downstream of the shock wave and therefore the decrease in the trailing edge pressure can be reduced when considerable suction effect is present which appears to be the case with results of Nagamatsu et al[1-3] and Krogamann et al[4].

The results for the integral value of stagnation pressure loss (Fig. 12c) show that the beneficial effect of passive control in reducing the overall losses is only at $M_{SO} > 1.3$ and forward facing holes are better suited than normal holes for reducing the losses. These observations are consistent with earlier experiments on a circular arc model[4].

The drag reductions $\Delta C_D = C_{DO} - C_D$ normalised with respect to C_{DO} where C_D is the drag coefficient based on wake traverse for the porous model and C_{DO} is the corresponding drag for the solid model are plotted against M_{SO} in Fig. 13. The drag reductions with passive control are about 10% at high shock Mach numbers which compares with reductions of 10% to 30% obtained in other experiments.

The discrepancies in results between the experiments done at Renssaelaer Polytechnic (RPI)[1-3] and Queen's University (QUB)[5,8], both of which were performed on a bump model may be due to two reasons. The experiments at RPI were conducted at a very low value of R_θ, estimated to be less than 3,000, whereas the experiments at QUB were conducted at values of R_θ of 5,700 and 10,000. In the former case the shock boundary layer interaction is essentially controlled by viscous forces whereas in the latter case the interaction is controlled by both viscous and inertia forces. It could be that the passive control is subjected to considerable scale effects. Another difference between the two experiments is that the ratios of hole diameter to boundary layer displacement thickness at the foot of the shock d/δ^* are different. It is estimated that in the RPI experiments $\frac{d}{\delta^*} \simeq 4$. The corresponding value in the experiments conducted at QUB was $\frac{d}{\delta^*} \simeq 1$. The ratio $\frac{d}{\delta^*}$ may be an important parameter to achieve considerable drag reduction.

The experiments conducted with bump models are not strictly comparable to those done with a lifting aerofoil with circulation. Even so it is difficult to explain some of the experiments on lifting aerofoil where the porosity was very low and the porous surface was downstream of the original shock.

4. Conclusions

Passive control boundary layer experiments were conducted on a wall mounted part section supercritical aerofoil at a boundary layer momentum thickness Reynolds number at the foot of the shock $R_\theta = 5,700$. The results were in general agreement with an earlier work on a circular arc model conducted at $R_\theta = 10,000$. Some of the results were in disagreement with the experiments of Nagamatsu et al[3] conducted on the same supercritical aerofoil model but at $R_\theta \simeq 3,000$. It is suggested that a detailed experiment on a large scale model should be conducted to fully understand the mechanism and the benefits of passive controlled shock boundary layer interaction.

References

1. Bahi, L., "Passive shock wave/boundary layer control from transonic supercritical aerofoil drag reduction". Ph.D. dissertation. Rensselaer Polytechnic Institute, New York. 1982.

2. Bahi, L., Ross, J.M. and Nagamatsu, T. "Passive shock wave/boundary layer control for transonic aerofoil drag reduction." AIAA-83-0137, 1983.

3. Nagamatsu, H.T., Dyer, R., Troy, N. and Ficarra, R.V. "Supercritical aerofoil drag reduction by passive shock wave/boundary layer control". AIAA-85-0207, 1985.

4. Krogamann, P., Stanewsky, E. and Theide, P., "Effect of suction on shock boundary layer interaction on shock induced separation". J. Aircraft, Vol. 22, 1985. pp. 37-42.

5. Raghunathan, S. and Mabey, D.G. "Passive shock wave/boundary layer control experiments on a circular arc model". AIAA-86-0285, 1986.

6. Raghunathan, S., "Mean and fluctuating measurements in a passive controlled shock boundary layer interaction". ICAS, London, Paper 1.2.3. 1986.

7. Raghunathan, S. Gray, J.L. and Cooper, R.K. "Effect of inclination of holes on passive shock wave boundary layer control". AIAA-87-0437, 1987.

8. Raghunathan, S. and Mabey, D.G. "Passive shock wave/boundary layer control on a wall mounted model". AIAA J. Vol. 25, No. 2. 1987 pp. 275 - 278.

9. Raghunathan, S. "Pressure fluctuation measurements with passive shock/boundary layer control". AIAA J. Vol. 25, No. 4, pp. 626 - 638.

10. Chen,S.L., Chow,Y.S., Van Dalsem,W.R. and Holst, T.L., "Computation of viscous transonic flow over porous aerofoils". AIAA-87-0359, 1987.

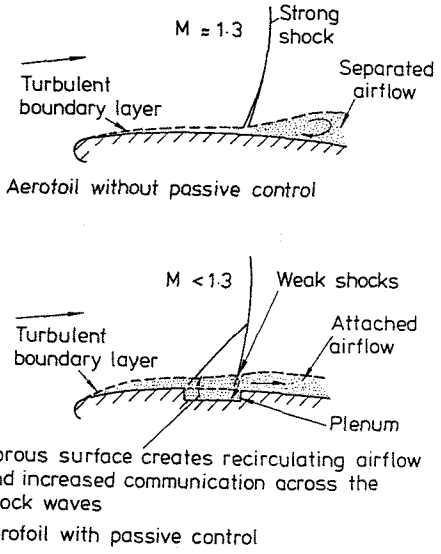

Fig. 1. Shock boundary layer interaction with and without passive control.

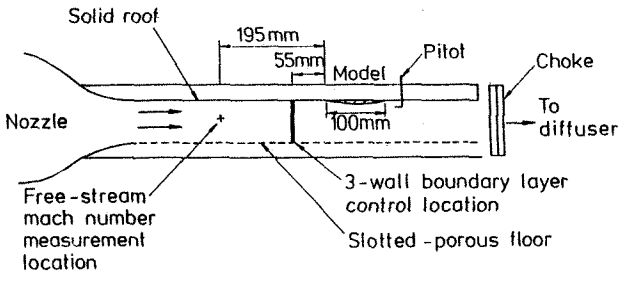

Fig. 2. Schematic diagram of the test setup.

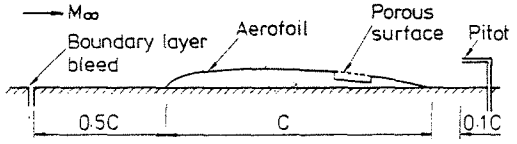

Fig. 3. Model details

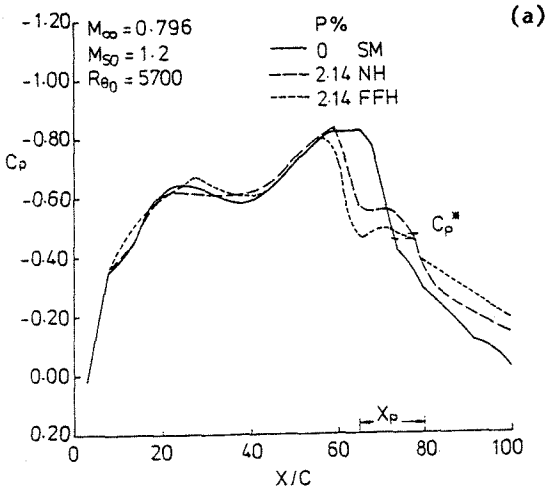

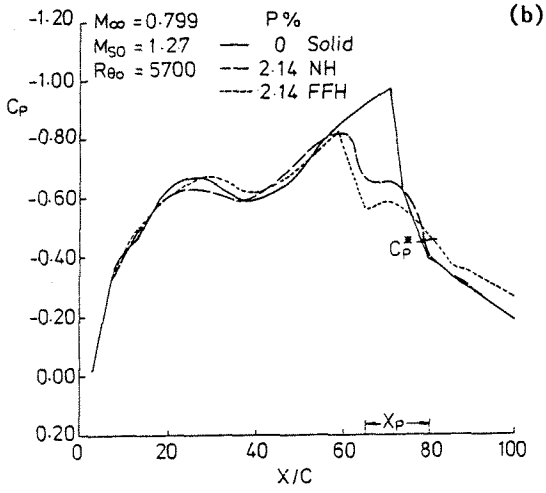

Fig. 4. Pressure distributions (a) M_{SO} = 1.2 (b) M_{SO} = 1.27

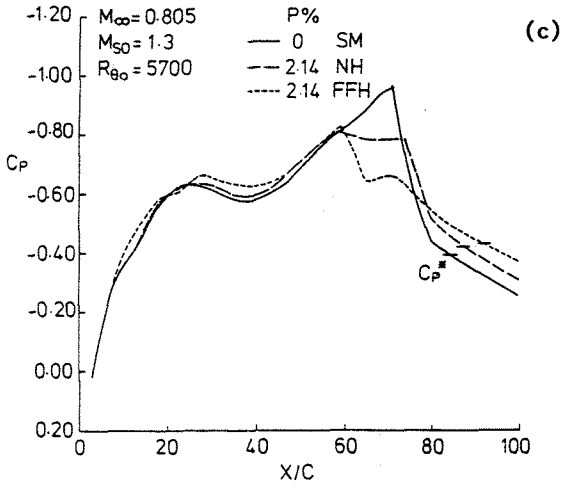

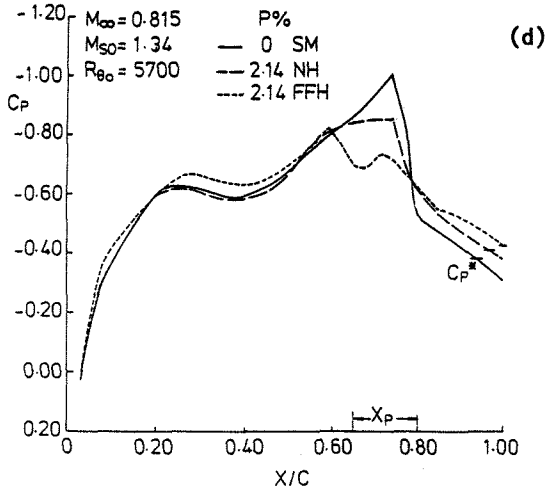

Fig. 4. Pressure distributions (c) M_{SO} = 1.3 (d) M_{SO} = 1.34

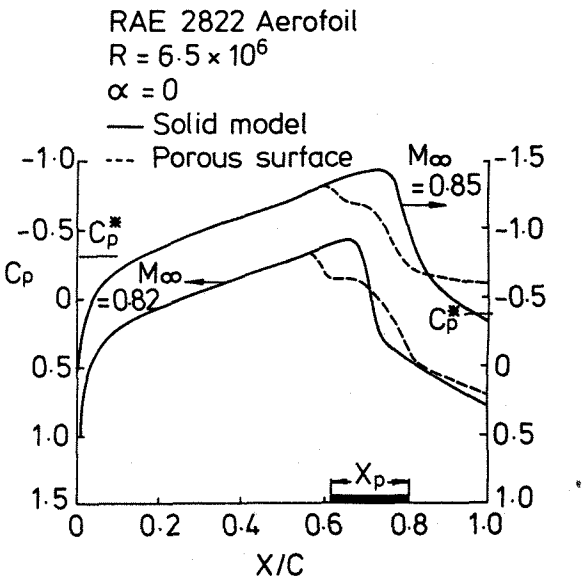

Fig. 5. Pressure distributions (theoretical) based on Ref. 10.

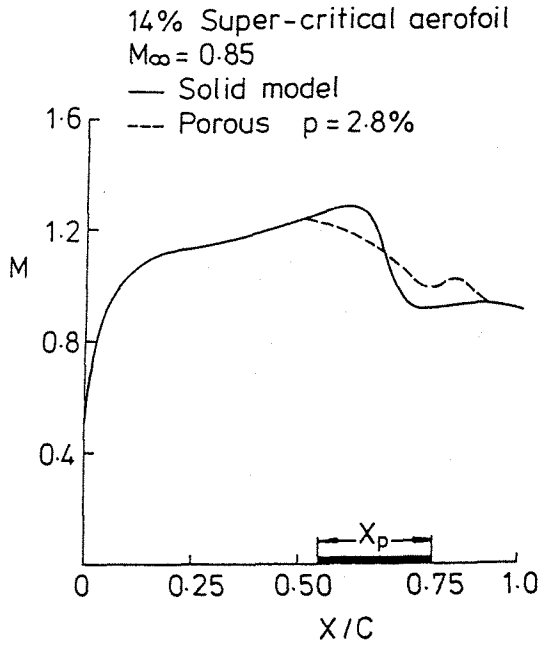

Fig. 6. Pressure distribution (experimental) from Ref. 2.

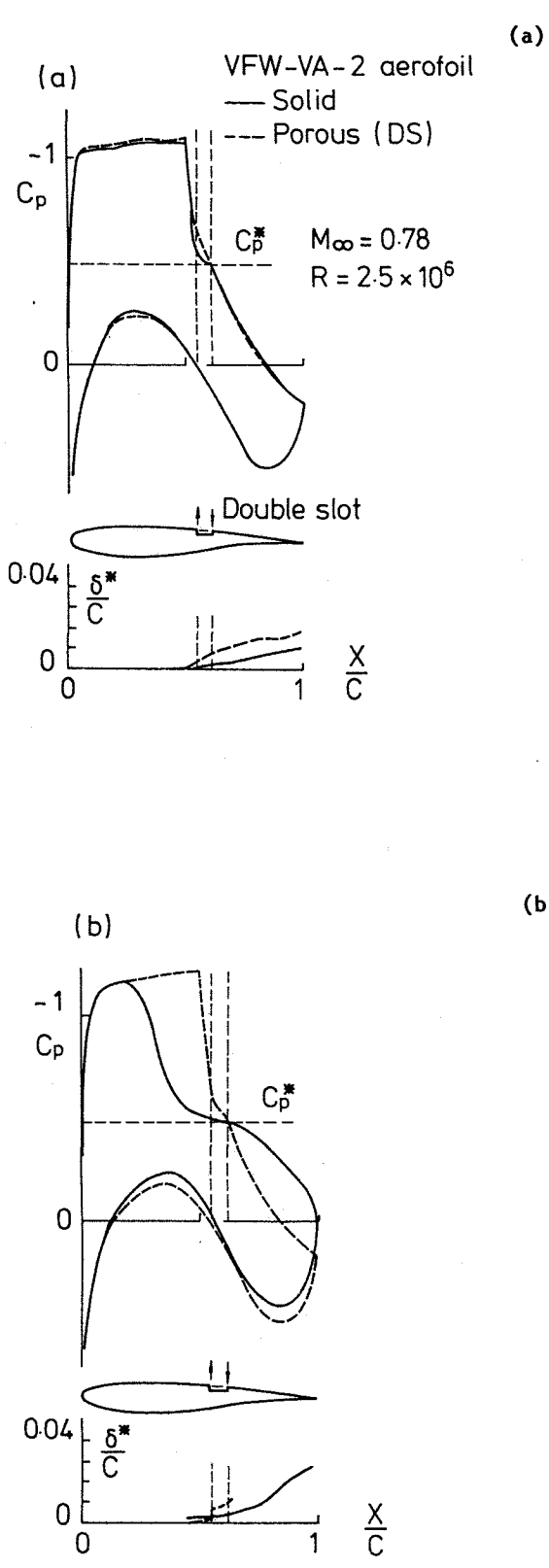

Fig. 7. Pressure distribution on an aerofoil with circulation (from Ref. 4).

(a) Passive control at the shock position.
(b) Passive control downstream of the original shock.

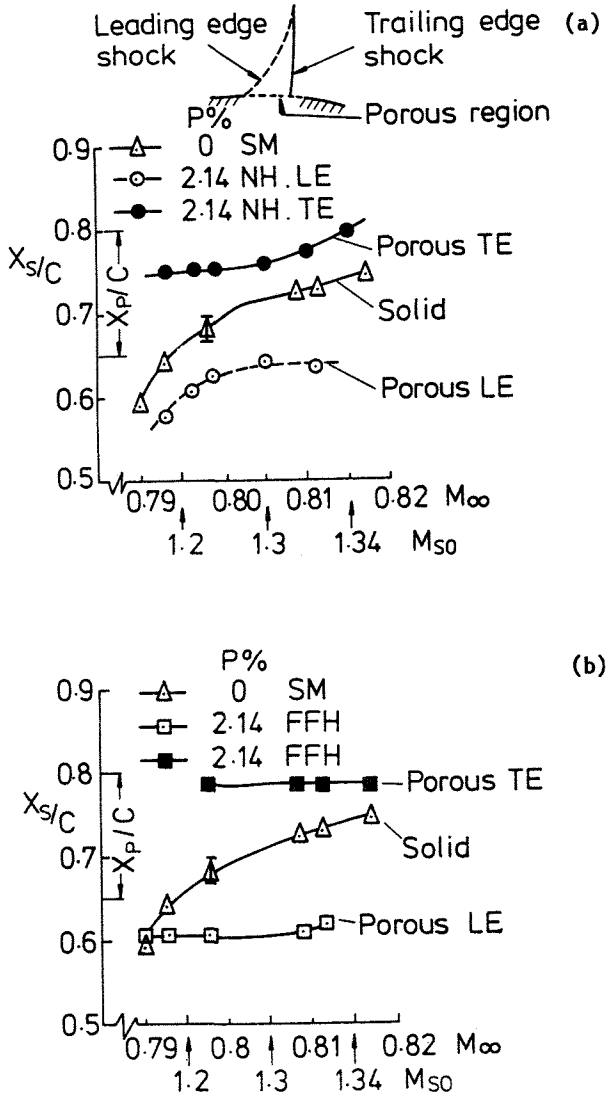

Fig. 8. Effect of passive control on shock position (a) Normal holes (b) Forward facing holes.

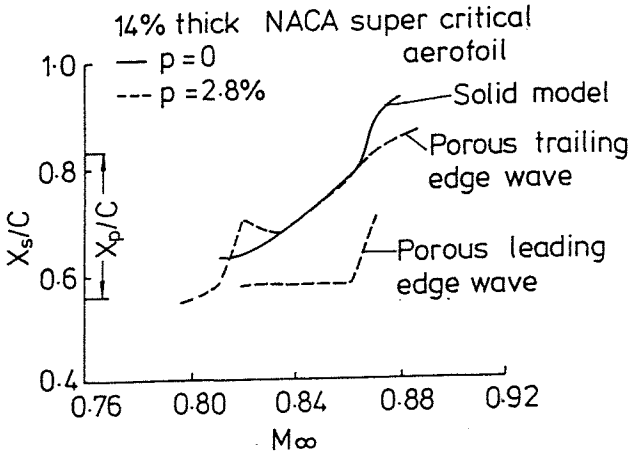

Fig. 9. Effect of passive control on shock position (from Ref. 3).

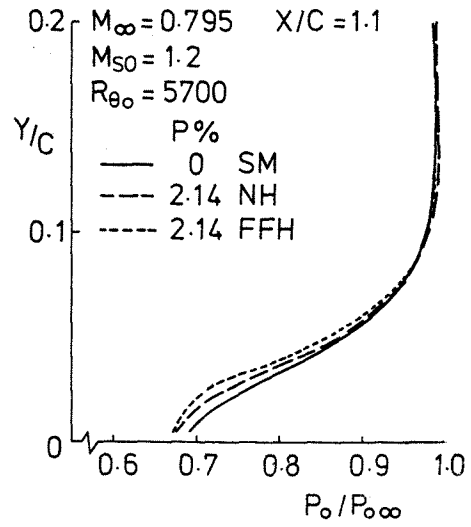

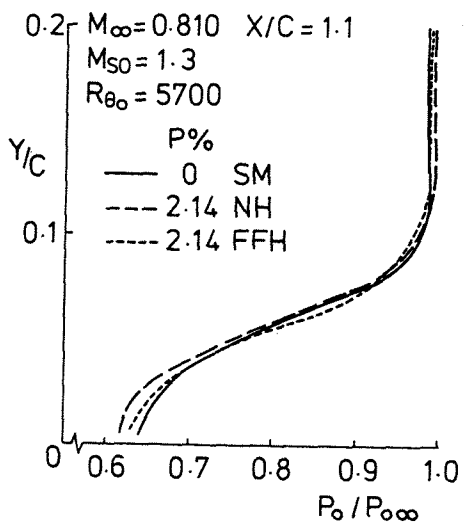

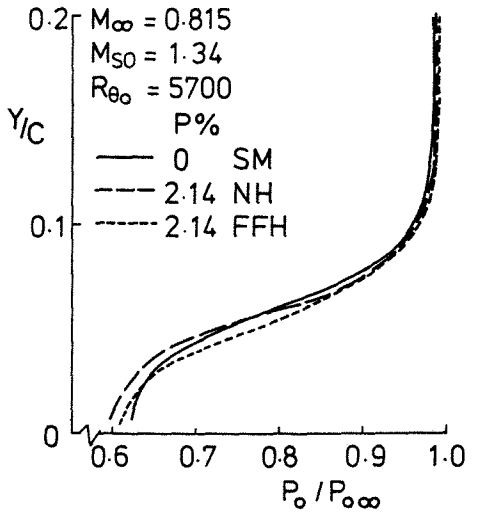

Fig. 10. Stagnation pressure profiles.
(a) $M_{SO} = 1.2$ (b) $M_{SO} = 1.3$ (c) $M_{SO} = 1.34$

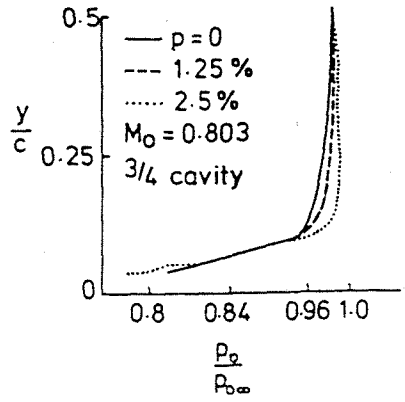

Fig. 11. Stagnation pressure profiles (from Ref. 1.)

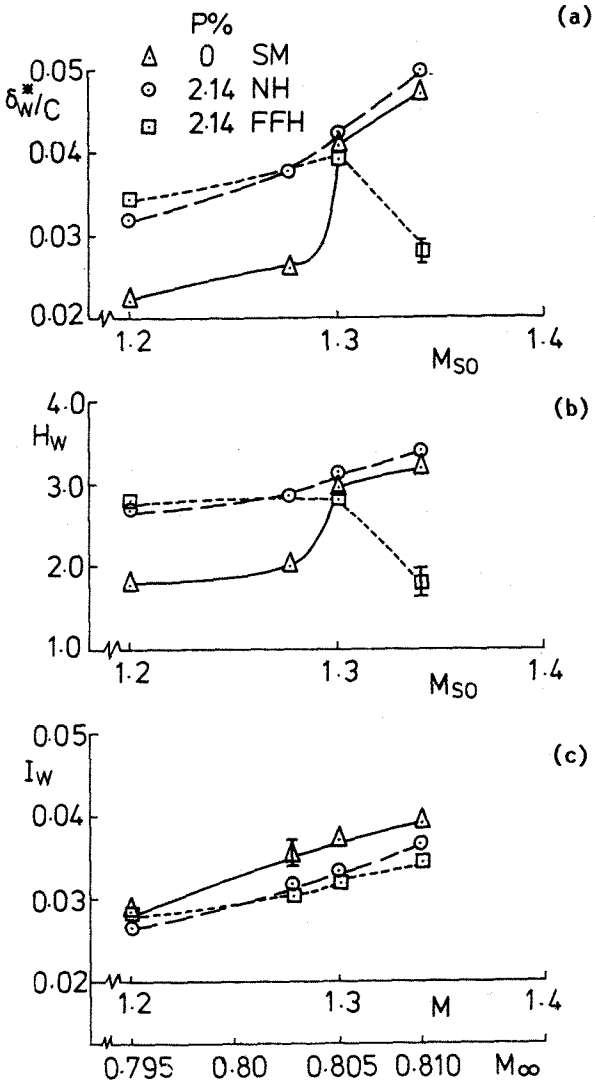

Fig. 12. Wake measurements
(a) Displacement thickness (b) Shape factor
(c) Stagnation pressure loss

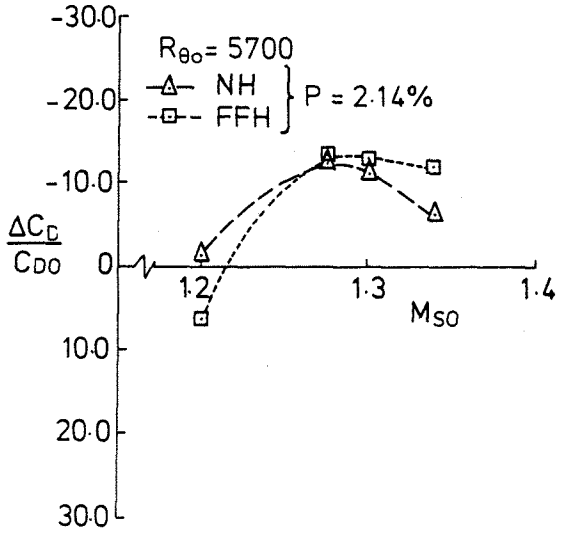

Fig. 13. Drag reduction with passive control